Crowdsourced Vertical Indoor Mapping

OMIDREZA MOSLEHIRAD[1], GEORGIOS PIPELIDIS[2], DOROTA IWASZCZUK[1], CHRISTIAN PREHOFER[2] & URS HUGENTOBLER[3]

Abstract: In this paper, we introduce a methodology for dynamic estimation of vertical features of buildings. For this, we obtain data from built-in smart-phone sensors and use this data for altitude estimation via the barometric formula. We propose a novel approach for the identification of the reference pressure during the outdoor-to-indoor-transition of the users. We use a set of machine learning algorithms for the determination of the number of floors as well as an unsupervised clustering of each floor altitude. This is the first system capable of mapping vertical features inside buildings automatically, which is independent of any indoor infrastructure. Finally, we apply the results for enhancing a CityGML standard for generating 3D building models.

1 Introduction

Indoor maps have many applications in e.g. robotics, augmented reality and location based services. Although there are proposed models for dynamic generation of indoor maps from crowdsourced data (GRZONKA et al. 2010; ALZANTOT & YOUSSEF 2012), no methodologies for vertical mapping using crowdsourced data exist. In this paper, we enhance existing models to include information regarding the number of floors and floor height. We also propose a novel approach for identifying reference locations via human transitions from outdoor to indoor, which can be used for a precise indoor altitude estimation. First, we use the crowdsourced smart-phone data to identify the user transition from outdoor to indoor. This serves as a landmark for the extraction of a reference pressure that can be used to estimate altitude differences via the barometric formula. Vertical transitions (e.g. stairs or elevators) are filtered out, since they do not belong to floors. The remaining altitude values from multiple users are aggregated for the identification of the number of floors and each floor height. Studies have attempted to vertically localize humans or objects via pressure sensors (BOLLMEYER et al. 2013; LI et al. 2013; XIA et al. 2015). However, they all assume that reference sensor stations are permanently installed in the buildings. These are thus highly infrastructure-dependent approaches. Approaches for the dynamic generation of maps have also been proposed (KIM et al. 2014; BOETERS et al. 2015; LOCH-DEHBI et al. 2017). However, these approaches use outdoor characteristics (e.g. windows, building footprints) to map indoor areas, which in most cases is not practical since most buildings contain indoor structures that are invisible from outside, including underground structures. This is also a problem for optical and microwave imagery techniques from airborne and spaceborne platforms,

[1] Technische Universität München, Lehrstuhl für Astronomische und Physikalische Geodäsie, Arcisstr. 21 D-80333 München, E-Mail: [omidreza.moslehi, dorota.iwaszczuk]@tum.de
[2] Technische Universität München, Fakultät für Informatik, Boltzmannstr. 3, D-85748 Garching, E-Mail: [georgios.pipelidis, christian.prehofer]@tum.de
[3] Technische Universität München, Forschungseinrichtung Satellitengeodäsie, Arcisstr. 21, D-80333 München, E-Mail: urs.hugentobler@tum.de

which are not able to easily sense deep internal geometries of buildings such as floors and their vertical locations.
In this paper, we present an approach for dynamic vertical mapping of building interiors using only crowdsourced smartphone data. In our method, we perform a self-calibration of the pressure sensor for every acquisition, which makes our method independent of permanently installed reference sensors. Presented work is a continuation of our previous research (PIPELIDIS et al. 2017). We extended the previous work for outdoor-indoor transition identification with image processing techniques such as Otsu's method, where we first convert the signals into one-dimensional gray images, then we perform image binarization via the Otsu's method to separate indoors from outdoors. We evaluated the results for not only three buildings, but seven different buildings. We also solved the open question of what if the user collects data only from indoor or only from outdoor, so we can determine if the collected dataset is from only indoor or outdoor.

2 Methodology

We collect data from smart-phone users via an application that is available here (PIPELIDIS 2017). We filter out the noise and outliers from the collected data. The next step is to filter out data from outdoors, leading to identification of areas where we extract indoor pressure readings. Following this, we filter features that belong to intermediate heights (i.e. stairs or elevators). The barometric formula is used for altitude estimation from pressure readings. We aggregate all altitude data from multiple visits of the targeted building, because the users often do not visit all the floors every time. The number of floors and every floor altitude are estimated from the aggregated datasets via clustering methods. We use this information to enhance indoor characteristics of CityGML model of buildings at lower levels of detail (LoD), presented as LoD2 Plus models.

2.1 Sensor Data Collection and Signal Filtering

We aim at fusion of all available smartphone data in order to get the best vertical mapping result. For this, we collect data from pressure, light, proximity, GPS and magnetic sensors. From the pressure sensor, we collect atmospheric pressure, which will be used for altitude determination via the barometric formula. The light sensor is sensitive to any light sources when the phone is outside of the pocket. It collects light values in the unit of lx, which measures the luminous flux per unit area. The proximity sensor produces a Boolean signal. If there is an object very close to it, the signal pattern will be changed to True. This is useful if during the data collection we want to know whether the phone is in a pocket or not, so if the phone is in the pocket, then the light sensor will not sense any light sources and the light signal will not be reliable at that period. From the GPS sensor, we calculate the Geolocation uncertainty of the user. The Geolocation uncertainty refers to the accuracy of user positioning via the GPS sensor in the unit of meter. Since the visibility of GPS sensors to GPS satellites is reduced inside buildings, the positioning accuracy will be reduced by several meters of error. From the magnetic sensor, we observe magnetic disturbances of the environment. In our study, we used data collected on different dates and at different day times, temperatures and humidity conditions. All the collected datasets are available in our public GitHub repository (MOSLEHIRAD 2017). For filtering out the outliers from

pressure signal, we used a third-order one-dimensional median filter (PRATT 2007). An exemplary pressure dataset is plotted in Fig. 1.

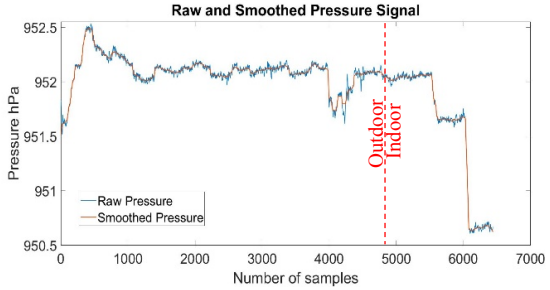

Fig. 1: Pressure sensor from outdoor and indoor. After the sample number 5000, the user entered into the building and visited three different floors: Ground, first and third floors, respectively.

2.2 Identification of Reference Pressure and Outdoor-Indoor Transition Point

The reference pressure is a big challenge for altitude estimation via the reformulation of the barometric formula $h = \left[\frac{P_0^{\frac{1}{5.25}}}{P_i} - 1\right] * \frac{T_b + 273.15}{0.0069}$, where, h is height, P_0 is the reference pressure extracted immediately after the transition point, P_i is the current pressure value and T_b is the temperature value obtained from the online weather stations. In our novel approach, we estimated P_0 from the outdoor-indoor transition of users instead of permanent installation of reference pressure sensors in buildings. For instance, after the stair-removal phase (Section 2.3), the first cluster of pressure samples are considered as the ground floor pressure samples, which we compute its mean as the reference pressure P_0. Another challenge is identification of the outdoor-indoor transition point itself. We fused built-in smart-phone sensors such as light, proximity, GPS and magnetic sensors since their signal patterns, in most cases, change significantly at transition points. In our data collection application, we modified the sampling frequency of these sensors for battery power management. In Fig. 2a, during the day, light intensity drops significantly at transition point and increases during the night, while the proximity sensor indicates whether to trust the light sensor, due to various phone poses (e.g. phone inside of pocket). In Fig. 2b, the Geolocation uncertainty pattern remained the same and is independent of day or night (always increases at transition point).

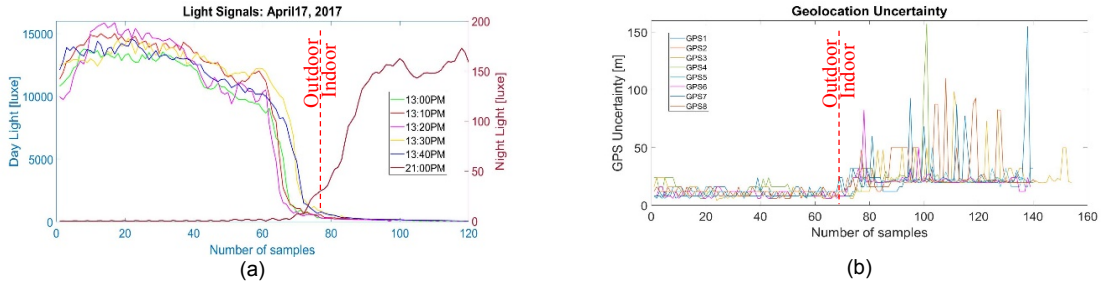

Fig. 2: Light and GPS Uncertainty data from several outdoor-indoor transitions

First, we smooth the light signal by the Gaussian filter (Fig. 3a) and convert it to a one-dimensional gray image. Afterwards, we convert it to a binary image via the Otsu's method (OTSU 1979), (Fig. 3b). If the data is from day time, an automatic gray threshold estimation for binarization is estimated, while for the night datasets, we consider a fixed empirical threshold of 10 lx. In order to have a uniform gray-scale for all the light datasets, we reduce all the samples

over the threshold of 2000 lx to 2000 lx. We selected this empirical threshold equivalent to the maximum gray-level of 255. In Fig. 3, an exemplary light dataset collected during a night is plotted.

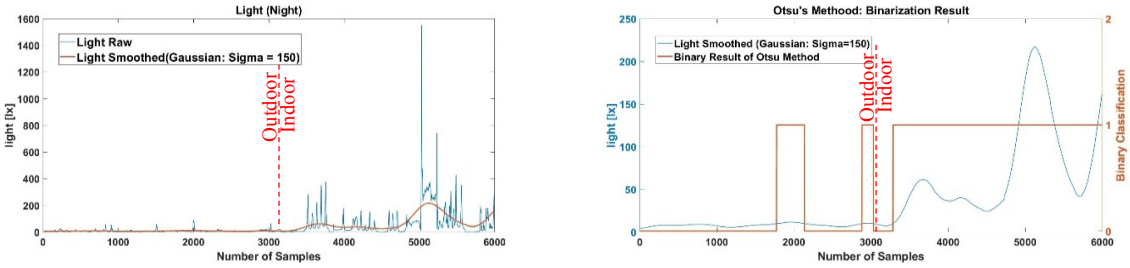

(a) (b)

Fig. 3: (a) A light data collected during a night and its smoothed signal. The user entered the building after the sample 3000. During this data collection, there were not sufficient light sources in the ground floor (samples from 3000 to 3500). (b) Binarization result via the Otsu's method

The reliability of light datasets during nights is lower than during the days, because during days, we always guarantee the Sun to be available outdoors, but we do not guarantee if there will be all necessary light sources available indoors. Besides, if the data is collected during the day, the light intensity contrast between indoors and outdoors is higher than during the night, which gives a better contrast for classification of indoors and outdoors. In above example, we considered the worst case: light dataset from night and when we entered the building, there were not sufficient light sources in the ground floor. However, we solved this problem by fusing multiple sensors. One of the main reasons why light datasets from night time are still useful for outdoor-indoor transition identification is the difference between received light intensity from light sources at different distances from the smart-phones. During the night, outdoors, artificial light sources have much higher distance from smart-phones than indoors (e.g. light bulbs at ceilings vs. light bulbs over streets). For instance, in Fig. 3a, the light samples from 0 to 3000 are from outdoor, which have very low intensity values than indoors during the night. Unlike artificial light sources, the Sun light is independent of distance from smart-phones and produces very high intensity values. Due to smoothing via the Gaussian filter, the identified transition points via the Otsu's method might be slightly displaced from the true locations. The other problem is the areas that wrongly identified as indoors (Fig. 3b, area around the sample number 2000). To solve these issues, we used Changepoint detection (LAVIELLE 2005) over the slightly smoothed light signal in Fig. 4a, where the mean of the signal changes significantly at change points, especially at the transition point (dashed green lines). This divides the signal into multiple segments. Finally, we use the Otsu's binary result as a weighting system for assignment of binary values to each segment (Fig. 4b). For example, the largest segment in Fig. 4b is over the samples 0 to 3462, where the mean of binary values of Otsu's result is lower than 0.5, so we assigned binary label of zero to all samples over this period, while for samples from 3462 to 5000, we have mean value of higher than 0.5, so we assigned binary label of one to all samples in this period. In our implementations, we assigned binary values of one to indoors and zero to outdoors. After applying the weights, the resulting final binary classification of light from night time can be seen in Fig. 4c.

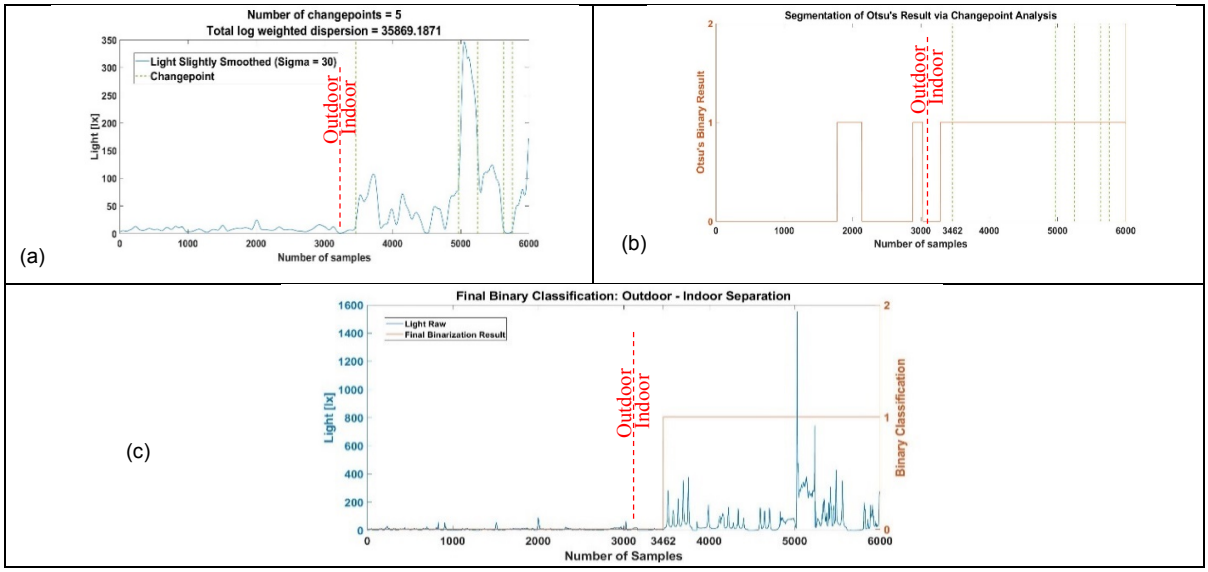

Fig. 4: (a) Changepoint analysis, where the signal is divided into 6 segments. (b) Segmentation of Otsu's result via mapping the change points over the Otsu's result. (c) Final binary classification of the light signal into indoor (binary values of ones) and outdoor areas (binary values of zeros)

However, in Fig. 4c, we are not sure if the sample number 3462 is exactly the transition point or not, because, as we mentioned before, after passing the true transition point (dashed red line), there were no sufficient light sources in the ground floor. Hence the point 3462 might be corresponding to the stairs or the next floor we visited after the ground floor. In order to find the correct transition point position, first we synchronized the light and Geolocation uncertainty signals based on their time dimension. Then we used the sudden increase of Geolocation uncertainty at the transition point as an additional indicator for a transition point (Fig. 5, dashed red line).

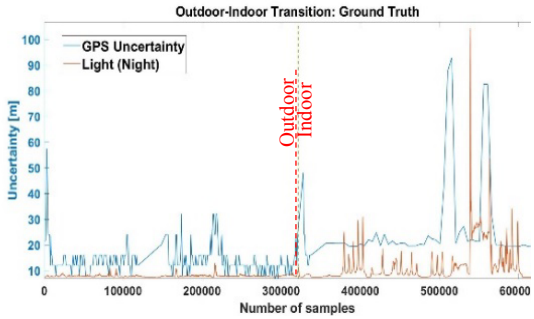

Fig. 5: The sudden rise in Geolocation uncertainty at transition point (at the dashed line) is used as an additional indicator of transition point. For synchronization, we resampled both the signals to the time unit of millisecond

For the GPS sensor, we used a similar approach. GPS is not accurate indoors due to the existence of walls and barriers, which results in a sudden increase of GPS uncertainty during outdoor-indoor transitions (Fig. 2b). First, we defined a bounding threshold of 70m to filter very high uncertainties, equivalent to a maximum gray-level of 255. Unlike the light signal where the threshold for binarization is calculated automatically, we used empirical uncertainty level equivalent to 13m, because the GPS uncertainty outdoors is usually below this level. In order to enhance the result of the Otsu's method, similar to the light signal, we perform the Changepoint detection analysis. As can be seen in Fig. 6b, the Changepoint analysis reduced number of outli-

ers significantly and helped to estimate the true transition point (sample 288). In the final binary classification of the Geolocation uncertainty, before the sample 288, there are only two small areas wrongly identified as indoors. As we mentioned before, we can remove the remaining outliers via fusion of multiple sensors.

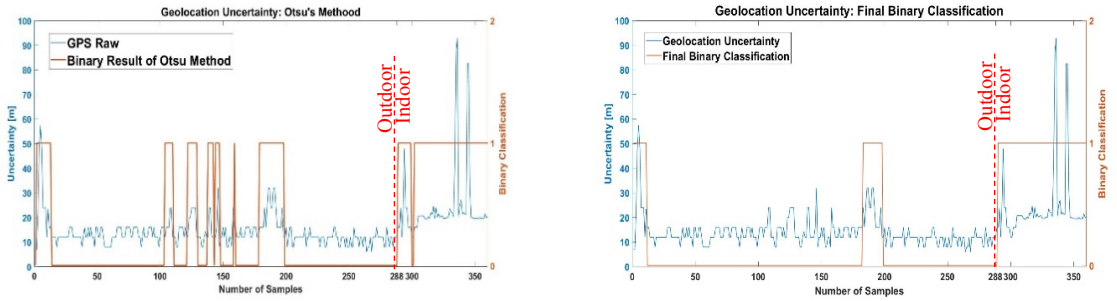

(a) (b)

Fig. 6: (a) Binarization result of the Geolocation uncertainty signal via the Otsu's method. (b) Final binary classification after segmentation of Otsu's binary result via the Changepoint analysis. The outlier around the sample number 200 is due to the presence of a bridge before the TUM Main Campus building entrance. This type of outliers can be removed via sensor fusion

In Fig. 7a, due to the existence of metallic structures and high electromagnetic variations indoors, we expect higher magnetic disturbances indoors than outdoors. In this figure, from the sample 5026, the user entered the building. First, we define a moving-standard-deviation window with a small size along the raw magnetic signal, which produces the first standard-deviation-signal (Fig. 7b). Following this, we define another moving-standard-deviation window, but with a larger size, to compute second-standard-deviation signal from the first one (Fig. 7c). Afterwards, we use Gaussian filter to smooth the second signal (Fig. 7d). This helps to increase the contrast between indoor and outdoor parts of the second standard-deviation signal. The mean value of the smoothed signal is used as the threshold for the binary classification of the magnetic signal into indoors and outdoors (Fig.7e). The first moving standard deviation normalizes the disturbances (Fig. 7b), while the second moving standard deviation is used to increase the amplitude of highly disturbed parts of the first moving standard deviation signal (Fig. 7c), which correspond to indoor areas.

At the end, we fused the binary results of all sensors to increase accuracy of outdoor-indoor binary classification result (Fig. 8). The fusion is based on what the majority of the sensors score (Tab. 1). For instance, if two out of three sensors score a sample as outdoor, then we label it as outdoor. If the proximity sensor indicates that the light signal is not available (phone in pocket) for a short period of time, then we ignore the light readings during that period and we rely only on GPS uncertainty signal, because fusion of GPS and Magnetic sensors does not improve accuracies (if we use only GPS sensor, it gives better results than fusion of these two).

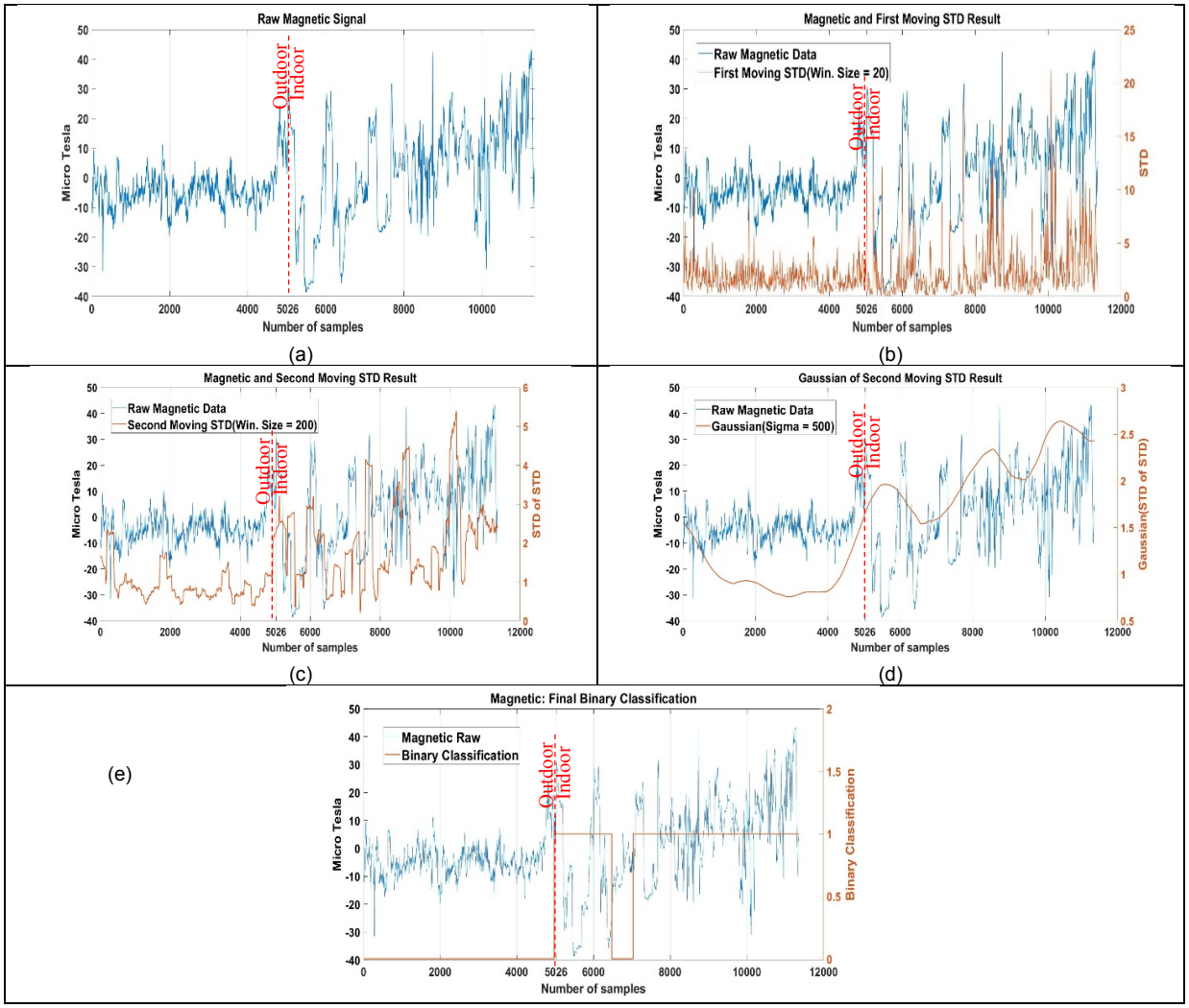

Fig. 7: (a) Magnetic disturbances from outdoor and indoor. From the sample 5026, the user entered a building. (b) The moving-standard-deviation algorithm applied over the raw magnetic signal with window size of 20. (c) Another moving-standard-deviation process, but with a larger window size of 200, which is applied over the previous moving-standard-deviation result obtained in b. (d) Gaussian smoothing of the resulting signal in c. (e) Final binary classification result

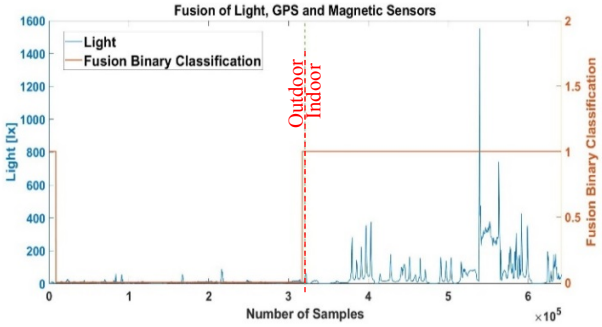

Fig. 8: Fusion result of multiple sensors. As can be seen in the figure, majority of indoor area is correctly labeled as indoor, while small section of the signal (start of the signal) is wrongly identified as indoor. The light signal is from night time and the dashed line is the true outdoor-indoor transition point

Tab.1: Truth table of our fusion concept for scoring what the majority of sensors indicate for outdoor-indoor transition identification. If the light signal is not available (phone in pocket), we rely only on GPS uncertainty.

Light	GPS	Magnetic	Fusion = Light ∧ (GPS ∨ Magnetic) ∨ (GPS ∧ Magnetic)	Indoor / Outdoor
F	F	F	F	Outdoor
F	F	T	F	Outdoor
F	T	F	F	Outdoor
F	T	T	T	Indoor
T	F	F	F	Outdoor
T	F	T	T	Indoor
T	T	F	T	Indoor
T	T	T	T	Indoor

In order to know if a light dataset is from day or night, we compute the maximum-bin-limit of its histogram. If this value is greater than or equal to 600, we consider it as a day dataset, and for values lower than 600, we assume it as a night dataset. If the user collects data only from indoor or only from outdoor, since we used image processing techniques, our approach will not fail. For example, Fig. 9 shows that if we collect light data during the day only from outdoor or only from indoor, our approach very accurately labels the entire signal as outdoor or indoor, respectively. In our approach, if the light signal is only from indoor, it mistakenly considers the dataset as a night dataset because its maximum-bin-limit becomes less than 600, so it applies fixed gray level of 10 lx for binarization. Since overall intensity of indoor light is usually much higher than 10 lx, the Otsu's method labels the entire signal as indoor (Fig. 9b). We also noticed that the light datasets are not reliable during the sunrise and sunset as the contrast between outdoor and indoor is not sufficient for binary classification via the Otsu's method. As a result, during these periods, we only rely on GPS uncertainty signal. To find out the sunrise or sunset periods, we can use the Sun angle with respect to the user's global coordination. There are online services that provide such information in real-time.

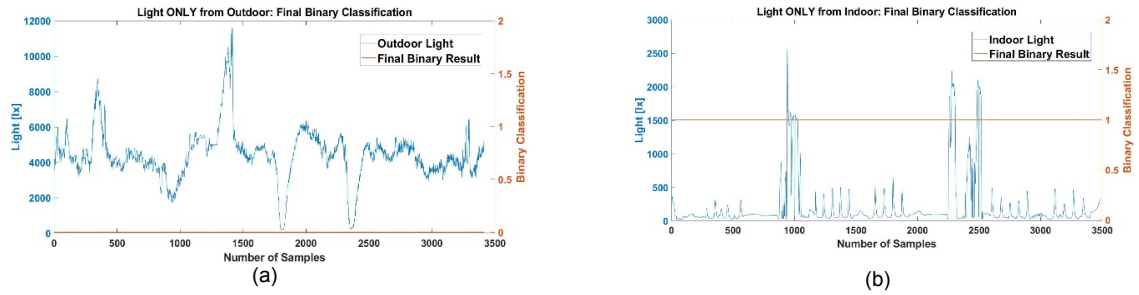

Fig. 9: Outdoor-indoor classification of light data only from outdoor or indoor, respectively

For the Geolocation uncertainty and magnetic signals, since they are not dependent on day or night, we do not have complexity of light data processing. For example, if we collect Geolocation uncertainty only from indoor or only outdoor, again our methodology works properly (Fig. 10).

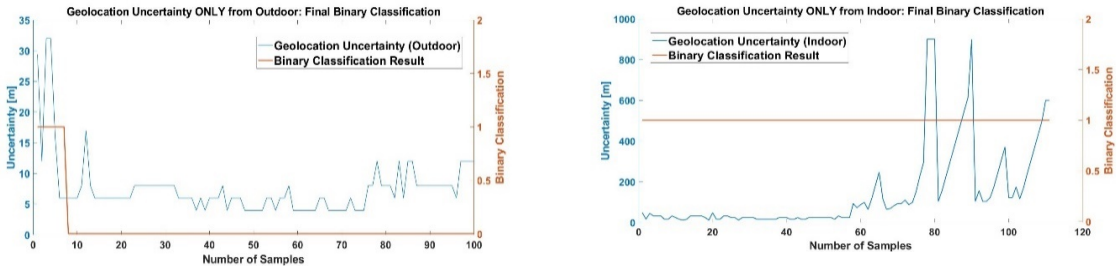

Fig. 10: Outdoor-indoor classification of Geolocation uncertainty data only from indoor or outdoor

2.3 Stair Removal

In the stair removal phase, we filter out data from stairs, elevators and outliers via the moving standard deviation algorithm. An exemplary result of this algorithm is shown in Fig. 11:

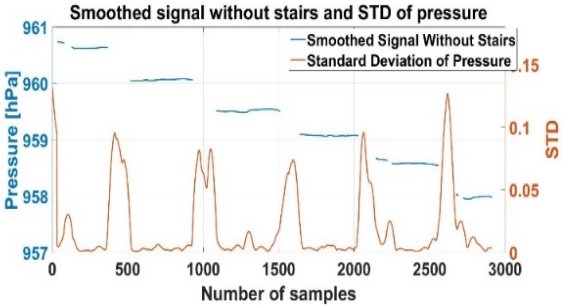

Fig. 11: Stair removal phase via the moving-standard-deviation algorithm. This algorithm filters out pressure readings from stairs and elevators. By setting a standard deviation threshold ($\sigma = 0.019$) and the sliding standard deviation window (size 28.5), we are able to remove pressure values with higher standard deviation than the threshold. At each movement, the algorithm computes the standard deviation of pressure values within the window. If the computed standard deviation is higher than the threshold, it filters out the corresponding pressure sample from the middle of the sliding window.

2.4 Number of Floors and Floor Altitude

After identification of floors pressure values via outdoor-indoor binary classification and stair removal phase, we estimated altitude values via the reformulation of the barometric formula in (Section 2.2). We aggregated multiple user altitude datasets, since not all users are expected to visit all floors. Since we extract the reference pressure by the same device we use for estimating floor altitude, unlike (XIA et al. 2015), there is no need for calibration between different barometric sensors. Since from the beginning the number of floors and their corresponding altitudes are unknown, for classification, we used K-Means because of its popularity and its relatively low processing demand and selected the Elbow method for estimating K (number of floors or clusters). The cluster centers represent the altitudes of the floors. In Fig. 12a, we presented a long-term pressure data collection from the TUM Main Campus Library building. We collected the datasets in 6 months, day and night, and in different weather conditions. Fig. 12b shows the altitude data aggregation of this building and the clustering result. In this figure, each color code corresponds to a specific floor, starting from ground floor to 5th floor (floors 0, 1, 2, 3, 4 and 5).

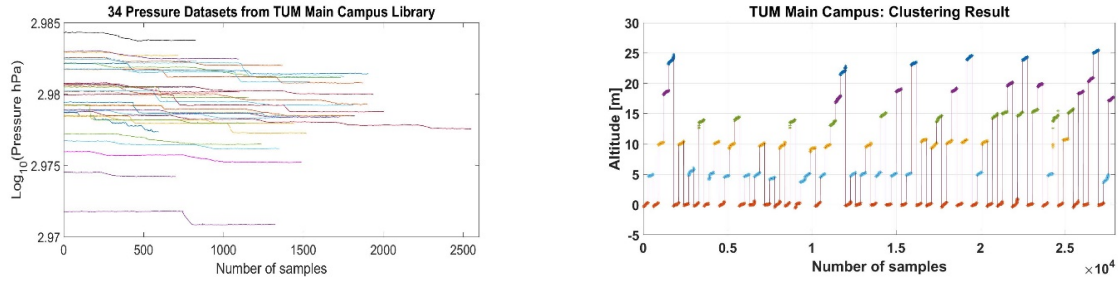

(a) (b)

Fig. 12: Pressure data collection and clustering result of aggregated altitude datasets.

2.5 CityGML LoD2 Plus Generator

We implemented a fully automatic CityGML LoD2 Plus building model generator via open tools and Java libraries such as Node-RED, citygml4j and OpenStreetMap queries, and visualized the models in a Virtual Reality environment using Unreal Engine. In another words, we insert raw sensor datasets as the input and obtain the corresponding building model as the output.

3 Evaluation

3.1 Data Collection Schedule

For evaluation of our proposed approach, we defined a long-term (six months) data collection schedule for each of the selected three buildings. We specified the floors to be visited in long-term period, day and night and in different weather conditions. For collecting each dataset, we walked about 800m outdoor and indoor, in total about 56km for all the collected datasets from all the buildings. The schedules can be found in (MOSLEHIRAD O. 2017), which describe all the details of collected datasets such as date, time, visited floors, temperature from AccuWeather (C°), temperature from the Weather Channel(C°), humidity from AccuWeather, humidity from the Weather Channel, ambient pressure from AccuWeather, ambient pressure from the Weather Channel, walking speed and cloud coverage. We wanted to know i.e. how the temperature, humidity or weather conditions can affect altitude readings in long-term visits of the buidings. At the end of the experiments, we noticed that the influence of temperature, humidity and weather variations have minor effects on the final floor altitude estimation results.

3.2 Influence of Different Phone Poses

All the evaluations are available in our public GitHub repository (MOSLEHIRAD 2017). A pre-study was conducted where the influence of different phone poses was estimated. These poses are: Phone (1) only in hand, (2) only in jacket pocket, (3) only in the swinging hand, (4) only in trouser pocket and (5) in a random assortment of above poses. We found that the influence on pressure due to different smart-phone poses is minor, with maximum vertical displacement of 40cm.

3.3 Influence of Stair Removal

We recorded data with three different walking velocities, approximately 1x, 1.5x and 2x, while climbing five flights of stairs in a building. The algorithm scores a precision of 93.8%, recall

95.5% and F-Score 94.6%, on correctly identifying the stairs, with the same moving standard deviation window length for all the data sets.

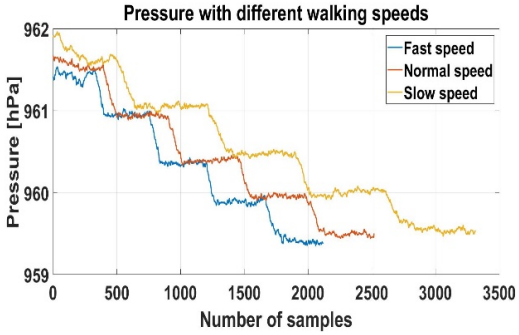

Fig. 13: Indoor pressure signals in three different walking speeds.

3.4 Evaluation of Reference Pressure Area (Outdoor – Indoor Transition)

We evaluated our approach for seven different buildings, each with four times visits for data collection during day and night. These buildings are located in Munich and the datasets as well as confusion matrices can be found in (MOSLEHIRAD 2017). Tab. 2 presents the accumulated binary classification result of all datasets from the seven buildings. According to the results, we can see that if the light is always available, we will have a better indoor area identification than GPS, magnetic and even fusion. However, light is not always available, so in this case, fusion gives a better reliability. Besides, fusion gives the best outdoor identification with true negative of 97,6% and precision of 98%, respectively. In terms of accuracy and F-Score, fusion comes after light, but as mentioned before, light is not always available. The less reliable sensor is the magnetic sensor since there are lots of magnetic noises outdoors, which affect the binary classification results.

Tab. 2: Total evaluation of outdoor-indoor transition via light, GPS and magnetic sensors and fusion result

	Recall	True Negative	Precision	Accuracy	F-Score
Light	97,3%	95,7%	96%	96,6%	96,7%
GPS	89,1%	93,4%	85,2%	92,1%	87,1%
Magnetic	84,1%	85,7%	85,1%	84,9%	84,6%
Fusion	94,5%	97,6%	98%	96%	96,2%

3.5 Evaluation of Number of Floors and Floor Altitude

We evaluated the estimated number of floors and floor altitude via 34, 25 and 20 datasets, collected form TUM Library, AO Laim and DeutschAkademie buildings, respectively, based on a schedule. We evaluated our approach based on monthly and total aggregation of altitude datasets. This helped us to compare the accuracy of partially or fully aggregated datasets. Fig. 14 (a, c and e) show the Elbow result for the three buildings. For instance, in (a), during April, the aggregated datasets for this month cover only the floors 0,1 and 2. The first K_{temp} after the threshold of 99.12% for this month is 2, and based on our implementation, we always increment K_{temp} by one to obtain the true K, which in this month is three (three visited floors). This threshold is given empirically and works correctly for all the datasets from all the buildings. All the selected buildings have the same number of floors (6 floors: Ground as **floor 0** to 6th floor as **floor 5**). As can be seen in Fig. 14 (b, d and f), the fully aggregated datasets result in a better floor altitude estimation as they are closer to the ground truth that is obtained via a laser range

meter. The error bars in (b), (d) and (f) are based on the standard deviation of each cluster. Tab. 3, 4 and 5 illustrate the ground truth, estimated floor altitude and absolute errors for the three buildings.

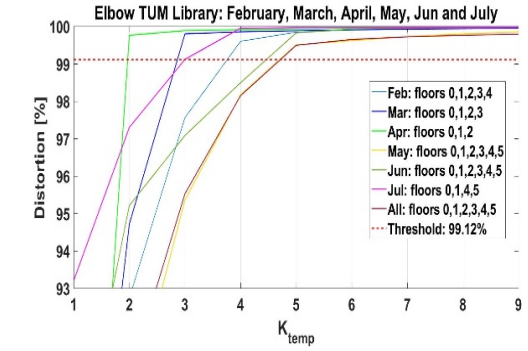

(a) TUM Elbow: Monthly and total data aggregation.

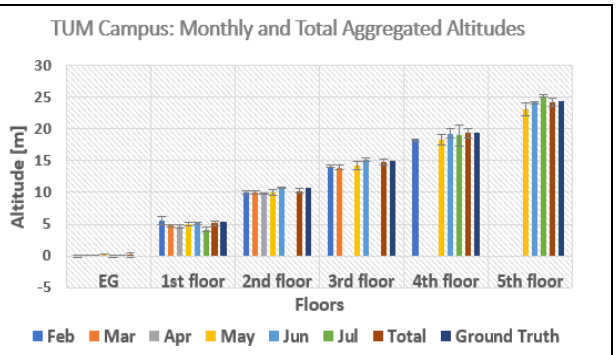

(b) TUM: Monthly and total of 34 dataset aggregation.

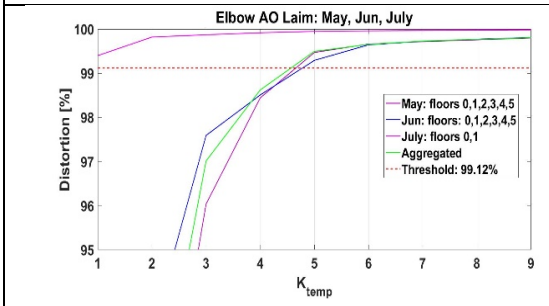

(c) AO Elbow: Monthly and total data aggregation.

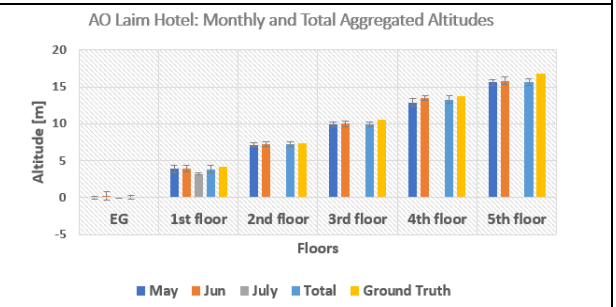

(d) AO: Monthly and total of 25 dataset aggregation.

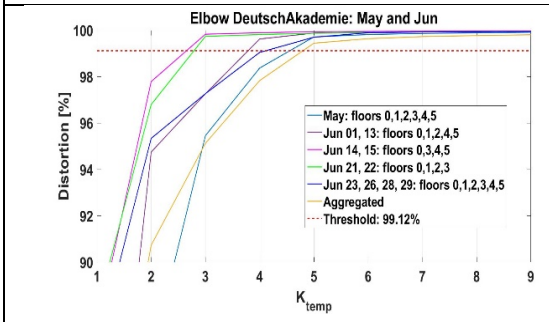

(e) De.Aka. Elbow: Monthly and total data aggregation.

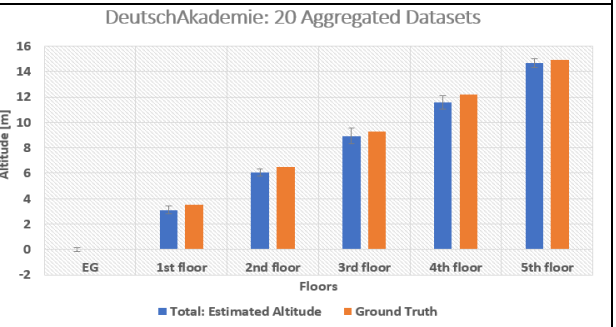

(f) DeutschAkademie: Total of 20 dataset aggregation.

Fig. 14: Evaluation of the number of floors and floor altitude for three different buildings

Tab. 3: Ground truth, estimated floor altitude and absolute errors for the TUM Main Campus building

Floors	Ground	First	Second	Third	Fourth	Fifth
True Altitude (m)	0	5,3	10,68	15,05	19,47	24,41
Estimated Altitude (m)	0	4,81	10,03	14,48	18,86	23,74
Absolute Error (m)	0	0,48	0,65	0,57	0,61	0,66

Tab. 4: Ground truth, estimated floor altitude and absolute errors for the AO Laim Hotel

Floors	Ground	First	Second	Third	Fourth	Fifth
True Altitude (m)	0	4,17	7,31	10,5	13,7	16,8
Estimated Altitude (m)	0,02	3,86	7,24	9,92	13,26	15,68
Absolute Error (m)	0	0,31	0,07	0,58	0,44	1,12

Tab. 5: Ground truth, estimated floor altitude and absolute errors for the DeutschAkademie building

Floors	Ground	First	Second	Third	Fourth	Fifth
True Altitude (m)	0	3,54	6,51	9,31	12,2	14,9
Estimated Altitude (m)	0	3,1	6	8,9	11,59	14,67
Absolute Error (m)	0	0,4	0,45	0,38	0,61	0,23

3.6 Generated CityGML LoD2+ Models and Demonstrations in VR

Fig. 15 shows our generated enhanced CityGML models (LoD2+) for a couple of buildings and representation of a model in VR environment. We used different tools such as citygml4j open java library, OpenStreetMap queries and Node-Red to automate the entire model generation process from sensor signals. Some of the demonstrations can be found in (VIDEO 01 & VIDEO 02).

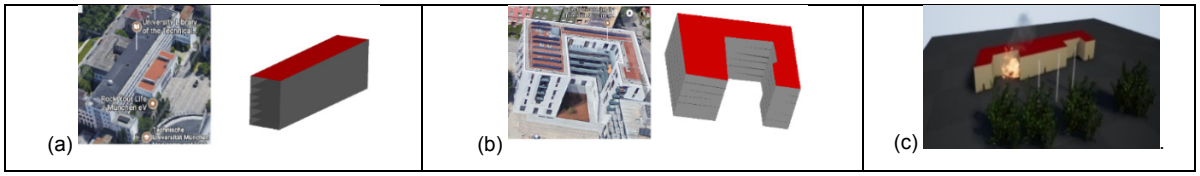

Fig. 15: CityGML LoD2 Plus models of TUM Main library, DeutschAkademie and VR visualization.

4 Conclusion and Future Work

This paper proposed our approach for the vertical mapping of buildings via crowdsourcing. We estimated each floor altitude via the barometric formula. For this, we introduced a novel approach for the extraction of reference pressure during the outdoor-to-indoor-transition of users, which is identified via sensor fusion. As a continuation of our previous work (PIPELIDIS et al. 2017), we proposed a different approach for outdoor-indoor transition identification: image-processing-based methods to have a more robust and general methodology. We evaluated the results for a higher number of buildings (seven buildings), while it was for only three buildings in the previous work. Thanks to the image processing algorithms and histogram analysis of the datasets, we solved the problem of what if the user collects data only from indoor or only from outdoor. In this scenario, we can determine if the user has been collecting data only from indoor or outdoor. Additionally, we solved an unsupervised classification problem, where the number of floors and the altitude of each floor were unknown. Finally, we proposed a way to map those characteristics by enhancing a CityGML building model and automated the whole process via the Node-RED. In future work, the intermediate reference pressures from each floor can improve the accuracy. Also reference pressure from multi-entrance buildings with different entrance levels is still an open question.

5 Literature

ALZANTOT, M. & YOUSSEF, M., 2012: UPTIME: Ubiquitous pedestrian tracking using mobile phones. IEEE Wireless Communications and Networking Conference (WCNC), 3204-3209.

BOETERS, R., OHORI, K.A., BILJECKI, F. & ZLATANOVA, S., 2015: Automatically enhancing citygml lod2 models with a corresponding indoor geometry. International Journal of Geographical Information Science, **29**(12), 2248-2268.

BOLLMEYER, C., ESEMANN, T., GEHRING, H. & HELLBRCK, H., 2013: Precise indoor altitude estimation based on differential barometric sensing for wireless medical applications. IEEE International Conference on Body Sensor Networks, 1-6.

GRZONKA, F., DIJOUX, A.; KARWATH, & BURGARD, B., 2010: Mapping indoor environments based on human activity, in Robotics and Automation (ICRA). IEEE International Conference on Robotics and Automation, 476-481.

KIM, J.S., YOO, S.J. & LI, K.J., 2014: Integrating IndoorGML and CityGML for Indoor Space. Springer Berlin Heidelberg, 184-196.

LAVIELLE M., 2005: Using penalized contrasts for the change-point problem. Signal Processing, **85**, 1501-1510.

LI, B., HARVEY, B. & GALLAGHER, T., 2013: Using barometers to determine the height for indoor positioning. International Conference on Indoor Positioning and Indoor Navigation, 1-7.

LOCH-DEHBI, S., DEHBI, Y. & PLMER, L., 2017: Estimation of 3d indoor models with constraint propagation and stochastic reasoning in the absence of indoor measurements. ISPRS International Journal of Geo-Information, **6**(3).

MOSLEHIRAD O., 2017: GitHub Repository. https://github.com/omidrad2017/Crowdsourced-vertical-indoor-mapping-Final.

OTSU, N., 1979: A Threshold Selection Method from Gray-Level Histograms. IEEE Transactions on Systems, Man, and Cybernetics, **9**(1), 62-66.

PIPELIDIS G., 2017: RecordData. https://play.google.com/store/apps/details?id=com. recordData.basic&hl=en.

PIPELIDIS, G., MOSLEHIRAD, O., IWASZCZUK, D., PREHOFER, C. & HUGENTOBLER, U., 2017: A novel approach for dynamic vertical indoor mapping through crowd-sourced smartphone sensor data. International Conference on Indoor Positioning and Indoor Navigation (IPIN), Sapporo, 1-8.

PRATT, W.K., 2007: Digital Image Processing 4th Ed. John Wiley & Sons, in Hoboken, NJ.

VIDEO 01: https://youtu.be/TPWhTybm5mA

VIDEO 02: https://www.youtube.com/watch?v=RwtW5eoYZO8&feature=youtu.be

XIA, H., WANG, X., QIAO, Y., JIAN, J. & CHANG, Y., 2015: Using multiple barometers to detect the floor location of smart phones with builtin barometric sensors for indoor positioning. Sensors, **15**(4), 7857-7877.